

An Analytic Solution to a Parameterized Problems Arising in Heat Transfer Equations by Optimal Homotopy Analysis Method

Hany Nasr HASSAN* and Mourad Samir SEMARY

Department of Basic Science, Faculty of Engineering, Benha University, Benha 13512, Egypt

(*Corresponding author’s e-mail: h_nasr77@yahoo.com)

Received: 21 September 2012, Revised: 2 June 2014, Accepted: 25 June 2014

Abstract

In this paper, an accurate approximate solutions for 2 problems arising in heat transfer straight fins are presented using optimal homotopy analysis method (OHAM). The approximated solutions are obtained at different values of parameters for the 2 problems are illustrated, and the fin efficiency is also evaluated. Moreover, the 2 problems are of nonlinear convective-radiative conduction and power-law fin-type. The obtained series solutions of OHAM are compared with the numerical solution (using Mathematica solver) and exact solutions. The square residual error is obtained to verify the accuracy of the presented method.

Keywords: Optimal homotopy analysis method, series solutions, fin efficiency, the square residual error, convergence-controller parameter.

Introduction

We consider the nonlinear 2 point boundary value problem;

$$\frac{d^2u}{dx^2} - \gamma^2u + \lambda \left(u \frac{d^2u}{dx^2} + \left(\frac{du}{dx} \right)^2 \right) - \beta u^4 = 0 \tag{1}$$

with boundary conditions;

$$u'(0) = 0, u(1) = 1 \tag{2}$$

where γ, λ, β are parameters. Eq. (1) contains 2 nonlinear problems arising in heat transfer equations. The first problem is called the nonlinear convective-radiative conduction problem is one dimensional heat transfer in a straight fin and the fin surface transfers heat through both convection and radiation, we consider $\lambda = \varepsilon_1, \beta = \varepsilon_2, \gamma = N$ and $u(x) = \theta(X)$ where ε_1 is the so-called thermal conductivity parameter, ε_2 is the thermal radiative parameter, N is the thermo-geometric fin parameter and $\theta(X)$ is the temperature distribution within the fin see [1,2], Eqs. (1) and (2) become;

$$\frac{d^2\theta}{dX^2} - N^2\theta + \varepsilon_1 \left(\theta \frac{d^2\theta}{dX^2} + \left(\frac{d\theta}{dX} \right)^2 \right) - \varepsilon_2\theta^4 = 0, \quad \theta'(0) = 0, \quad \theta(1) = 1. \tag{3}$$

The second problem called the power-law fin-type problem is a one-dimensional steady-state heat conduction equation for the temperature distribution along a straight fin with the nonlinearity of high

order if $\lambda = \gamma = 0$ and $\beta = \varepsilon$ where ε is the convective-conductive parameter of the fin and $u(x) = \theta(x)$ see [3,4], Eqs. (1) and (2) become;

$$\frac{d^2\theta}{dx^2} - \varepsilon\theta^4 = 0, \quad \theta'(0) = 0, \quad \theta(1) = 1. \tag{4}$$

Fins are very frequently encountered in many engineering applications to enhance heat transfer between a solid surface and its convective, radiative, or convective radiative surface, fins are used in air conditioning, air-cooled craft engines, refrigeration, cooling of computer processors, cooling of oil carrying pipe lines etc. Most engineering problems, especially some heat transfer equations are nonlinear, and in most cases it is difficult to solve them, especially analytically, so these equations may be approximated using semi-analytical techniques such as the differential transform method (DTM) [1], homotopy perturbation method (HPM) [2,3], the Adomian's decomposition method (ADM) [5,6], and variational iteration method (VIM) [7]. However, these methods cannot provide us with a simple way to adjust and control the convergence region and rate of giving approximate series. Therefore in this work, the problem (1) solved for different values of the parameters γ, λ and β using the optimal homotopy analysis method (OHAM). The homotopy analysis method (HAM) initially proposed by Liao in his Ph.D. thesis [8] was proposed to get analytical approximations of highly nonlinear equations. The HAM can guarantee the convergence of the series solutions by auxiliary parameters especially the so-called convergence-controller parameter \hbar [9,10]. In recent years, HAM and its modifications have been successfully employed to solve many types of nonlinear problems in science and engineering [11-21].

Materials and methods

Analysis of method

Consider the nonlinear 2 boundary value problems in finite domain;

$$u''(x) + f(u, u') = g(x), \tag{5}$$

with boundary conditions;

$$u'(0) = A, \quad u(1) = B, \tag{6}$$

$f(u, u')$ is the nonlinear function, and $g(x)$ is the non-homogeneous term, the Eq. (5) becomes;

$$\bar{N}[u(x)] - g(x) = 0. \tag{7}$$

where \bar{N} is a nonlinear operator, x denote independent variable, and $u(x)$ is an unknown function. The first step in this method adds the new condition $u(0) = \alpha$ or $u'(1) = \alpha$ where α is unknown and will determine later, then the boundary conditions (6) become;

$$u'(0) = A, \quad u(0) = \alpha. \tag{8}$$

or

$$u(1) = B, \quad u'(1) = \alpha. \tag{9}$$

The other boundary conditions $u(1) = B$ in Eq. (8) or $u'(0) = A$ in Eq. (9) use to obtain as a function of convergence-controller parameter h , we construct the general zero-order deformation equation as follows;

$$(1-p)L[\phi(x, \alpha, p) - u_0(x)] = p\hbar H(x)(\bar{N}[\phi(x, \alpha, p)] - g(x)) . \tag{10}$$

Where denote the so-called embedding parameter. $\hbar \neq 0$ is an auxiliary parameter, L is an auxiliary linear operator. The HAM is based on a kind of continuous mapping $u(x, \alpha) \rightarrow \phi(x, \alpha, p)$; $\phi(x, \alpha, p)$ is an unknown function, $u_0(x, \alpha)$ is an initial guess of $u(x, \alpha)$ and $H(x)$ denotes a non-zero auxiliary function. It is obvious that when the embedding parameter $p = 0$ and $p = 1$, Eq. (10) becomes;

$$\phi(x, \alpha, 0) = u_0(x, \alpha) , \phi(x, \alpha, 1) = u(x, \alpha). \tag{11}$$

respectively. Thus as p increases from 0 to 1, the solution $\phi(x, \alpha, p)$ varies from the initial guess $u_0(x, \alpha)$ to the solution $u(x, \alpha)$. Expanding $\phi(x, \alpha, p)$ in the Taylor series with respect to p , one has;

$$\phi(x, \alpha, p) = u_0(x, \alpha) + \sum_{m=1}^{+\infty} u_m(x, \alpha) p^m , \tag{12}$$

where

$$u_m(x, \alpha) = \frac{1}{m!} \left. \frac{\partial^m \phi(x, \alpha, p)}{\partial p^m} \right|_{p=0} , \tag{13}$$

The initial guess $u_0(x, \alpha)$ of the solution $u(x, \alpha)$ can be determined by the rule of solution expression as follows. From Eq. (5), with the new boundary condition Eq. (8) or Eq. (9), the solution $u(x, \alpha)$ expressed by a set of base functions;

$$\{(x-c)^n | n = 0, 1, 2, 3, \dots\} , c = 0 \text{ or } 1. \tag{14}$$

In the form;

$$u(x, \alpha) = \sum_{n=0}^{+\infty} f_n(\alpha)(x-c)^n . \tag{15}$$

The initial guess $u_0(x, \alpha)$ can be chosen from Eq. (15) so that it achieves the boundary condition Eq. (8) or Eq. (9).

The second goal is to determine the higher order terms $u_m(x, \alpha)(m, 1, 2, \dots)$. Define the vector;

$$\bar{u}_i(x) = \{u_0(x), u_1(x), \dots, u_i(x)\}. \tag{16}$$

Differentiating Eq. (10) m times with respect to the embedding parameter p and then setting $p = 0$ and finally dividing them by $m!$. We have the so-called m th-order deformation equation;

$$L[u_m(x, \alpha) - \chi_m u_{m-1}(x, \alpha)] = p\hbar H(x)R(\bar{u}_{m-1}), \tag{17}$$

and its boundary condition Eq. (18) or Eq. (19) for the new boundary conditions Eq. (8) and Eq. (9) respectively;

$$u'_m(0) = 0, u_m(0) = 0, \tag{18}$$

$$u_m(1) = 0, u'_m(1) = 0, m \geq 1. \tag{19}$$

where

$$R(\bar{u}_{m-1}) = \frac{1}{m-1!} \frac{\partial^{m-1}(\bar{N}[\phi(x, \alpha, p)] - g(x))}{\partial p^{m-1}} \Bigg|_{p=0}, \tag{20}$$

and

$$\chi_m = \begin{cases} 0 & \text{when } m \leq 1 \\ 1 & \text{otherwise} \end{cases} \tag{21}$$

Now the solution of the *m*th-order deformation Eq. (17) for $m \geq 1$ when $H(x) = 1$ becomes;

$$u_m(x, \alpha) = \chi_m u_{m-1}(x, \alpha) + L^{-1}(p\hbar R(\bar{u}_{m-1})). \tag{22}$$

then

$$u(x, \alpha) \cong U_M(x, \alpha, \hbar) = \sum_{m=0}^M u_m(x, \alpha, \hbar). \tag{23}$$

The third goal is to determine the optimal value of convergence-controller parameter \hbar , from Eq. (23) and unused boundary conditions from Eq. (6) in new boundary condition Eq. (8) and Eq. (9), it $u(1) = B$ or $u'(0) = A$, we can find the relation between the convergence-control parameter \hbar and α ;

$$U_M(1, \alpha, \hbar) = B, \tag{24}$$

or

$$U'_M(0, \alpha, \hbar) = A. \tag{25}$$

By plotting the Eq. (24) or Eq. (25) given the set R_\hbar for the convergence-control parameter that where the value of constant α . And using any \hbar belongs to R_\hbar one can get a convergent series solution. However, the convergence rate is also dependent upon \hbar but the so-called \hbar -curve approach cannot give the ‘‘optimal’’ value of \hbar in R_\hbar . One can define the exact square residual error Δ_M .

$$\Delta_M = \int_0^1 (\bar{N}(U_M(x, \alpha, \hbar) - g(x)))^2 dx, \tag{26}$$

However, more and more CPU time is needed to calculate the exact square residual error Δ_M , especially for large M , because Δ_M containing two unknown parameters α and \hbar therefore we can use the so-called averaged residual error [24] defined by;

$$E_M = \frac{1}{k} \sum_{s=0}^k \left(\bar{N}(U_M(s\Delta x, \alpha, \hbar) - g(s\Delta x)) \right)^2. \tag{27}$$

The minimum averaged residual error is given by a nonlinear algebraic equation;

$$\frac{\partial E_M}{\partial \hbar} = 0, \tag{28}$$

The new approach get the optimal value of convergence-controller parameter \hbar by solving Eq. (24) or Eq. (25) and Eq. (28). We will use this new approach to solve the nonlinear problem Eq. (1) at large different values of the parameters γ, λ and β .

Method implementation

We can consider the problem Eq. (1) with the new boundary condition according to Eq. (8) as follows;

$$\frac{d^2 u}{dx^2} - \gamma^2 u + \lambda \left(u \frac{d^2 u}{dx^2} + \left(\frac{du}{dx} \right)^2 \right) - \beta u^4 = 0, u(0) = \alpha, u'(0) = 0. \tag{29}$$

We choose the auxiliary linear operator;

$$L[\phi(x, \alpha, p)] = \frac{\partial^2 \phi(x, \alpha, p)}{\partial x^2}, \tag{30}$$

with the property;

$$L[c_0 + c_1 x] = 0, \tag{31}$$

$$\bar{N}[\phi(x, \alpha, p)] = \frac{\partial^2 \phi}{\partial x^2} - \gamma^2 \phi + \lambda \left(\phi \frac{\partial^2 \phi}{\partial x^2} + \left(\frac{\partial \phi}{\partial x} \right)^2 \right) - \beta \phi^4, \tag{32}$$

and

$$R_m(\bar{u}_{m-1}) = \frac{d^2 \bar{u}_{m-1}}{dx^2} - \gamma^2 \bar{u}_{m-1} + \lambda \left(\sum_{i=0}^{m-1} u''_i \bar{u}_{m-1-i} + u'_i u'_{m-1-i} \right) - \beta \sum_{i=0}^{m-1} \sum_{j=0}^i \sum_{k=0}^j \bar{u}_{m-1-i} \bar{u}_{i-j} \bar{u}_{j-k} \bar{u}_k, \tag{33}$$

The solution of the m th-order deformation Eq. (22) for $m \geq 1$;

$$u_m(x, \alpha) = \chi_m u_{m-1}(x, \alpha) + \hbar \int \int R_m(\bar{u}_{m-1}) dx dx + c_0 + c_1 x. \tag{34}$$

where the integration constants c_0 and c_1 are determined by the boundary conditions according to Eq. (18);

$$u_m(0) = 0, u'_m(0) = 0. \tag{35}$$

We choose only initial guess $u_0(x, \alpha)$ imposed according to the initial condition Eq. (29) and Eq. (15).

$$u_0(x, \alpha) = \alpha. \tag{36}$$

Eqs. (34) and (35) can be easily solved using computational software such as Mathematica. For example the solution of Eq. (34) at $m = 1$ is;

$$u_1(x, \hbar, \alpha, \gamma, \lambda, \beta) = -\hbar x^2 \left(\frac{\gamma^2 \alpha}{2} + \frac{\beta \alpha^4}{2} \right), \tag{37}$$

$u_m(x, \hbar, \alpha)$ ($m = 2, 3, 4, \dots$) can be calculated similarly. Hence the series solution is;

$$\begin{aligned} u(x) &= u_0 + u_1 + u_2 + u_3 + \dots \\ &= \alpha + \left(\begin{array}{l} -2\hbar \alpha^4 \beta - 2\hbar \alpha \gamma^2 - \frac{3}{2} \hbar^2 \alpha (\alpha^3 \beta + \gamma^2) (1 + \alpha \lambda) \\ -\hbar^2 \alpha (\alpha^3 \beta + \gamma^2) (1 + \alpha \lambda) (1 + \hbar + \hbar \alpha \lambda) \\ -\frac{1}{2} \hbar^2 \alpha (\alpha^3 \beta + \gamma^2) (1 + \alpha \lambda) (1 + \hbar + \hbar \alpha \lambda)^2 + \dots \end{array} \right) x^2 \\ &\quad + \left(\begin{array}{l} \frac{1}{8} \hbar^2 \alpha (\alpha^3 \beta + \gamma^2) (4\alpha^3 \beta + \gamma^2) \\ + \frac{1}{12} \hbar^2 \alpha (\alpha^3 \beta + \gamma^2) (4\alpha^3 (\beta + 2\hbar \beta) + (1 + 2\hbar) \gamma^2 + 11\hbar \alpha^4 \beta \lambda + 5\hbar \alpha \gamma^2 \lambda) \\ + \frac{1}{24} \hbar^2 \alpha (\alpha^3 \beta + \gamma^2) (4(1 + 4\hbar + 3\hbar^2) \alpha^3 \beta + (1 + 4\hbar + 3\hbar^2) \gamma^2 \\ + 11\hbar(2 + 3\hbar) \alpha^4 \beta \lambda + 5\hbar(2 + 3\hbar) \alpha \gamma^2 \lambda + 21\hbar^2 \alpha^5 \beta \lambda^2 + 12\hbar^2 \alpha^2 \gamma^2 \lambda^2) + \dots \end{array} \right) x^4 + \dots \end{aligned} \tag{38}$$

The approximation solution $U_M(x, \hbar, \alpha, \gamma, \lambda, \beta)$ to the strong nonlinear problem Eq. (29);

$$U_M(x, \hbar, \alpha, \gamma, \lambda, \beta) = \sum_{m=0}^M u_m(x, \hbar, \alpha, \gamma, \lambda, \beta). \tag{39}$$

The relation between the convergence-control parameter \hbar and α , using the boundary condition $u(1) = 1$ in Eq. (39), it becomes;

$$u(1) \cong U_M(1, \hbar, \alpha, \gamma, \lambda, \beta) = 1. \tag{40}$$

Finding the value of $\alpha = u(0)$ and the optimal value of the convergence-control parameter \hbar , by solving Eq. (40) and Eq. (28).

Results and discussion

Case (1)

If $\lambda = \varepsilon_1, \beta = \varepsilon_2, \gamma = N$ and $u(x) = \theta(X)$ then problem Eq. (1) becomes Eq. (41) known as the nonlinear convective-radiative conduction equation;

$$\frac{d^2\theta}{dX^2} - N^2\theta + \varepsilon_1 \left(\theta \frac{d^2\theta}{dX^2} + \left(\frac{d\theta}{dX} \right)^2 \right) - \varepsilon_2\theta^4 = 0, \theta'(0) = 0, \theta(1) = 1. \tag{41}$$

The approximation solution $\theta(X)$ to Eq. (41) from Eq. (39) becomes;

$$\theta(X) = U_M(X, \hbar, \alpha, N, \varepsilon_1, \varepsilon_2) = \sum_{m=0}^M u_m(X, \hbar, \alpha, N, \varepsilon_1, \varepsilon_2). \tag{42}$$

And from Eq. (40) the relation between $\alpha = \theta(0)$ and the convergence-control parameter \hbar becomes;

$$\theta(1) \cong U_M(1, \hbar, \alpha, N, \varepsilon_1, \varepsilon_2) = 1. \tag{43}$$

Recently, many authors have taken into consideration different values of $\varepsilon_1, \varepsilon_2, N$ in Eq. (41) and solved using different methods such as DTM [1], HPM [2], Galerkin Method (GM) [23], and traditional homotopy analysis method [24], but in this study we successfully solved the nonlinear problem Eq. (41) by the OHAM at larger values of parameters $\varepsilon_1, \varepsilon_2$ and N compared with the numerical solution (Mathematica solver) and evaluate the fin efficiency η prescribed in [1];

$$\eta = \int_0^1 \theta(X) dX. \tag{44}$$

Figure 1 is $\alpha - \hbar$ curve of Eq. (43) for small values of the parameters $\varepsilon_1, \varepsilon_2$ at $\varepsilon_1 = \varepsilon_2 = 0.2, N = 1$ for different M th-orders of approximation, it is easy to discover the valid region of $\hbar (R_h)$ that corresponds to the line segment nearly parallel to the horizontal axis (constant α value) but not get the optimal value from **Figure 1**, we can find this value by solving the Eq. (43) and Eq. (28). **Table 1** shows a solution for Eqs. (43) and (28) for 5th, 8th and 10th order of approximation, one can see the difference between the value of $\alpha = \theta(0)$ obtaining the used method and numerical value decreasing as the number of the order of approximation M increasing and the value of α at 10th order best of Galerkin method (GM) [23] and DTM [1], one can see in **Table 1** the square residual error Δ_M decreases with increase order of approximation M and also approaching to zero, this means increasing order of approximation M , the solution convergence to the numerical solution. This indicates the accuracy of the used method. The obtained efficiency value for fin η (44) in this case 0.775077.

Figures 2 - 6 are $\alpha - \hbar$ curves of Eq. (43) for different values of the parameters $\varepsilon_1, \varepsilon_2$ and N at the 15th order of approximation, we find the value $\alpha = \theta(0)$ and the optimal value of \hbar summarized in **Tables 2 - 6**, one can see these tables find the square residual error $\Delta_M \cong 0$ and **Figures 7 - 11** temperature distribution $\theta(X)$ when the used method is compared with numerical solutions. This indicates the high efficiency of the used method. The fin efficiency η is summarized in **Tables 2 - 6** for

different values of parameters $\varepsilon_1, \varepsilon_2$ and N , the fin efficiency decreases when the thermal radiative parameter ε_2 increases see **Tables 2 - 4**, but the fin efficiency increases when the thermal conductivity parameter ε_1 increases see **Tables 5** and **6**. Also by comparing **Tables 2 - 4** and **Tables 5** and **6** with each other we see that the fin efficiency η decreases when the thermo-geometric fin parameter N increases.

Table 1 Solving Eq. (43) and Eq. (44) for different M th - order approximation and compared by different methods.

$K = 10, N = 1, \varepsilon_1 = \varepsilon_2 = 0.2$			
order of approximation (M)	h	$\alpha = \theta(0)$	Δ_M (26)
5	-0.9401	0.6669748	1.007×10^{-7}
8	-0.8705	0.66701341	1.834×10^{-13}
10	-0.8810	0.667013361	4.7393×10^{-14}
Numerical solution		0.667013363	
DTM solution [1]		0.667013379	
GM solution [25]		0.6670130	

Table 2 The fin efficiency and the square residual error at $N = 0.5, \varepsilon_1 = 0.5$ and different values of ε_2 .

$M = 15, K = 10, N = 0.5, \varepsilon_1 = 0.5$					
$\alpha = \theta(0)$					
ε_2	Numerical	Used method (OHAM)	h	Δ_M (26)	η (44)
0.5	0.83212549	0.832155	-0.6958	4.750×10^{-19}	0.886712
2	0.70546201	0.7054620	-0.6057	4.021×10^{-14}	0.796767
4	0.62306445	0.6230645	-0.6403	1.854×10^{-14}	0.735078
10	0.50882308	0.5088231	-0.8954	4.5480×10^{-13}	0.643575
15	0.45967979	0.4596798	-0.9905	1.506×10^{-12}	0.6014069
30	0.3810879	0.3810875	-1.2561	1.212×10^{-8}	0.529360
80	0.285558	0.2855652	-1.4580	0.0000317	0.431816

Table 3 The fin efficiency and the square residual error at $N = 2, \varepsilon_1 = 0.5$ and different values of ε_2 .

$M = 15, K = 10, N = 2, \varepsilon_1 = 0.5$					
$\alpha = \theta(0)$					
ε_2	Numerical	Used method (OHAM)	h	Δ_M (26)	η (44)
0.5	0.33423	0.3342288	-0.7300	6.902×10^{-8}	0.544332
2	0.322051	0.3220484	-0.8506	6.430×10^{-8}	0.531863
10	0.2800092	0.2800065	-0.6938	2.680×10^{-7}	0.486521
50	0.20568	0.2057039	-1.0249	0.00204	0.395974
80	0.18256	0.1824	-1.2082	0.011	0.363973

Table 4 The fin efficiency and the square residual error at $N = 3$, $\varepsilon_1 = 0.5$ and different values of ε_2 .

$M = 15, K = 10, N = 3, \varepsilon_1 = 0.5$					
$\alpha = \theta(0)$					
ε_2	Numerical	Used method (OHAM)	\hbar	Δ_M (26)	η (44)
0.5	0.132143	0.1321785	-0.7469	0.0000396	0.381078
10	0.122076	0.1221183	-0.7265	0.000109	0.361655
80	0.091136	0.0908703	-1.0883	0.072	0.295483

Table 5 The fin efficiency and the square residual error at $N = 0.5$, $\varepsilon_2 = 0.5$ and different values of ε_1 .

$M = 15, K = 10, N = 0.5, \varepsilon_2 = 0.5$					
$\alpha = \theta(0)$					
ε_1	Numerical	Used method (OHAM)	\hbar	Δ_M (26)	η (44)
2	0.8995948701	0.89959487	-0.3684	3.282×10^{-16}	0.932819
4	0.934650779	0.93465078	-0.2150	3.712×10^{-18}	0.956372
10	0.968067559	0.96806756	-0.08714	3.880×10^{-20}	0.978705
15	0.977605679	0.97760568	-0.0478	1.49×10^{-17}	0.985068

Table 6 The fin efficiency and the square residual error at $N = 2$, $\varepsilon_2 = 0.5$ and different values of ε_1 .

$M = 15, K = 10, N = 2, \varepsilon_2 = 0.5$					
$\alpha = \theta(0)$					
ε_1	Numerical	Used method (OHAM)	\hbar	Δ_M (26)	η (44)
2	0.51134	0.5114584	-0.2910	0.000056	0.677030
4	0.652804	0.6528261	-0.1168	0.000133	0.771608
10	0.8185743	0.8185747	-0.0962	6.643×10^{-9}	0.880155
15	0.87060389	0.8706039	-0.0717	1.090×10^{-11}	0.914329

Figures 7 - 9 show temperature distribution $\theta(X)$ obtained from the used method and numerical solutions for different values of ε_2, N . **Figure 7** depicts the effect of the thermal radiative parameter ε_2 on temperature at $N = 0.5, \varepsilon_1 = 0.5$. The tip end temperature and mean temperature decrease when the thermal radiative parameter ε_2 increases. Also by comparing **Figures 7 - 9** we see that the tip end temperature decreases and the mean temperature when the thermo-geometric fin parameter N increases. **Figures 10 and 11** shows temperature distribution $\theta(X)$ obtained from the used method and numerical solutions for different values of ε_1, N . **Figure 10** depicts the effect of the thermal conductivity parameter ε_1 on temperature at $N = 0.5, \varepsilon_2 = 0.5$. The tip end temperature and mean temperature increases when the thermal conductivity parameter ε_1 increases. Also by comparing **Figures 10 and 11** we see the tip end temperature and mean temperature decrease when the thermo-geometric fin parameter N increases.

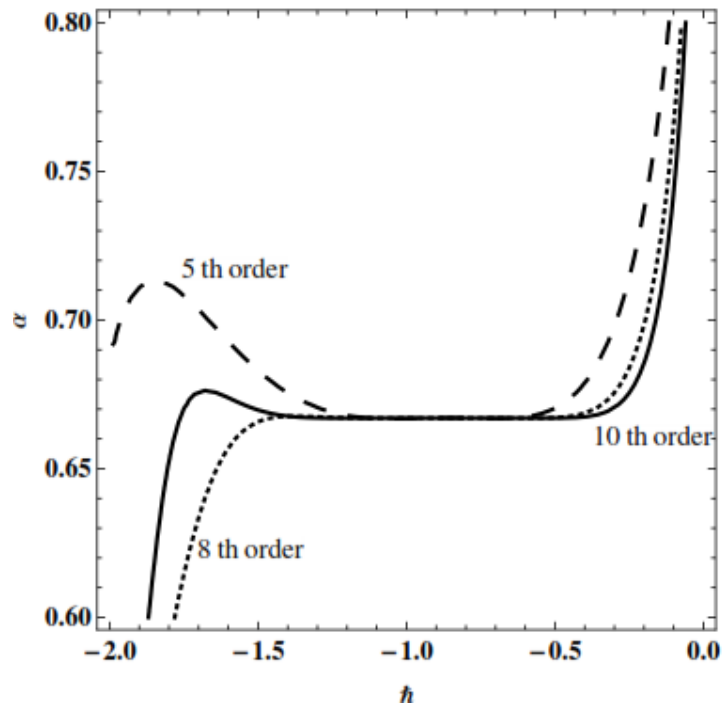


Figure 1 $\alpha - h$ curves of Eq. (43) at $\varepsilon_1 = \varepsilon_2 = 0.2, N = 1$ for different M th-order of approximation.

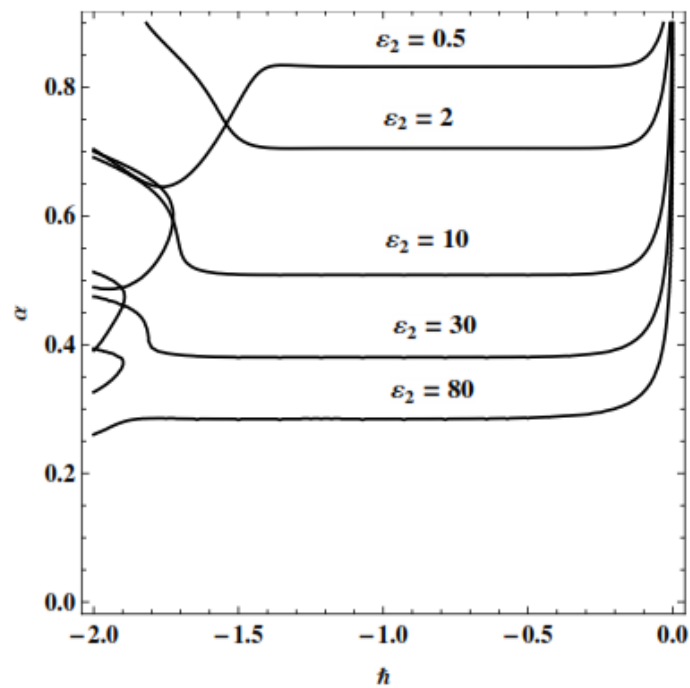


Figure 2 $\alpha - h$ curves of Eq. (43) at $\varepsilon_1 = 0.5, N = 0.5$ and $M = 15$ for different values of ε_2 .

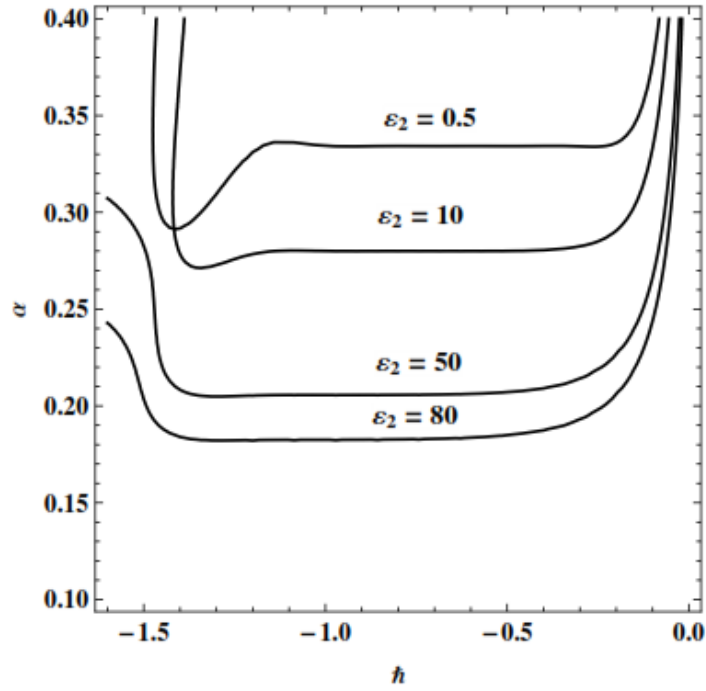


Figure 3 $\alpha - \hbar$ curves of Eq. (43) at $\varepsilon_1 = 0.5, N = 2$ and $M = 15$ for different values of ε_2 .

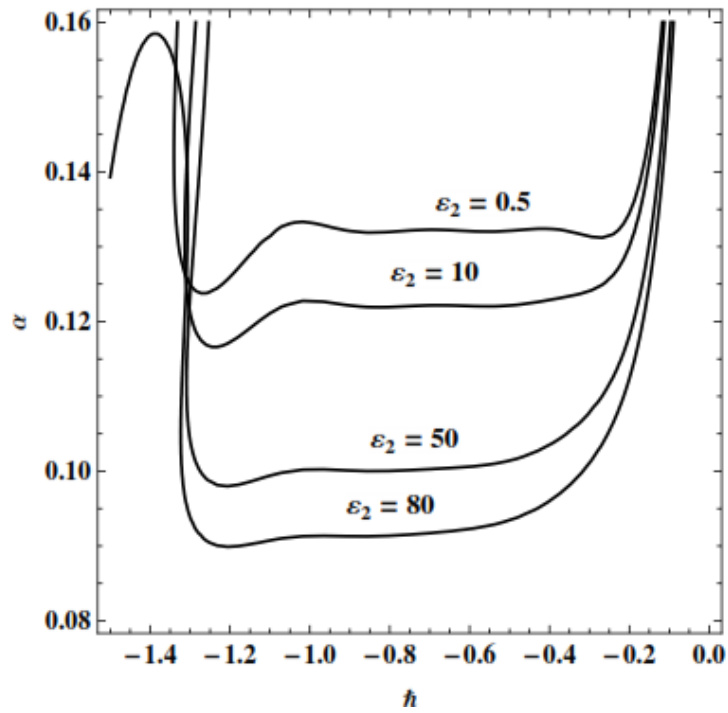


Figure 4 $\alpha - \hbar$ curves of Eq. (43) at $\varepsilon_1 = 0.5, N = 3$ and $M = 15$ for different values of ε_2 .

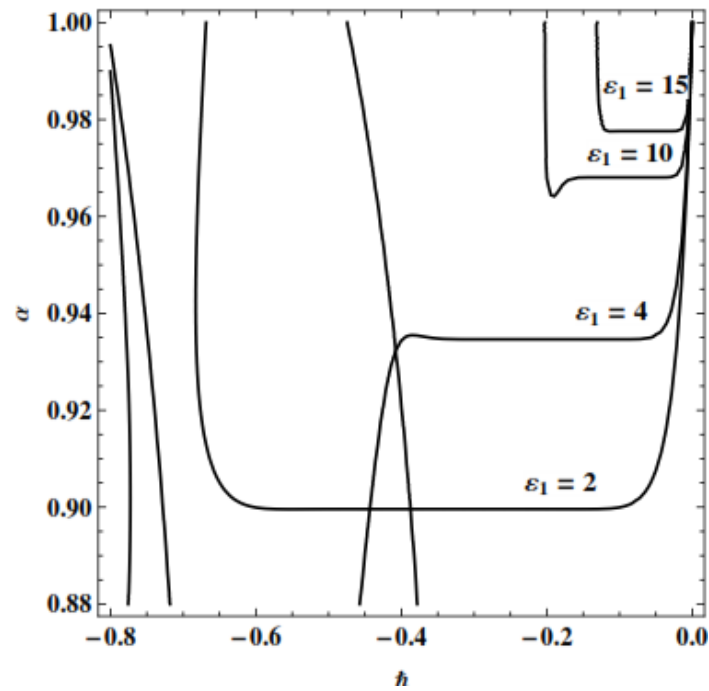


Figure 5 $\alpha - h$ curves of Eq. (43) at $\varepsilon_2 = 0.5, N = 0.5$ and $M = 15$ for different values of ε_1 .

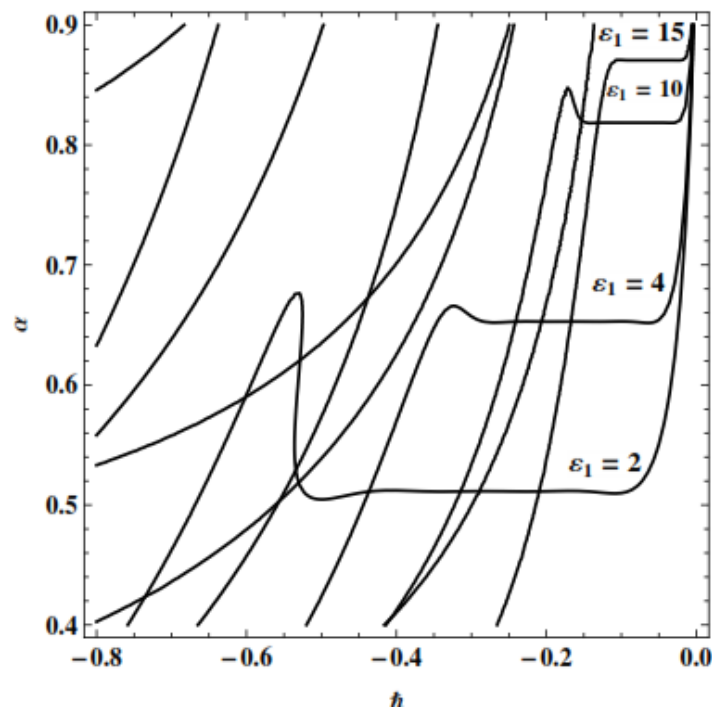


Figure 6 $\alpha - h$ curves of Eq. (43) at $\varepsilon_2 = 0.5, N = 2$ and $M = 15$ for different values of ε_1 .

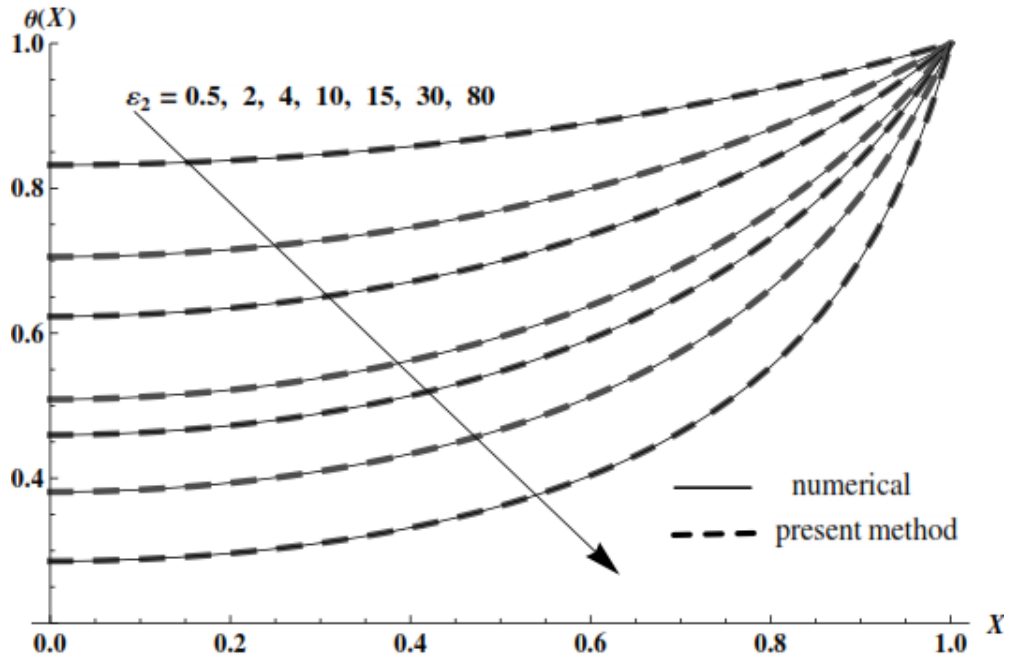


Figure 7 Comparison between the solutions from the used method and numerical solutions for $\theta(X)$ at $N = 0.5$, $\varepsilon_1 = 0.5$, $M = 15$ and different values of ε_2 .

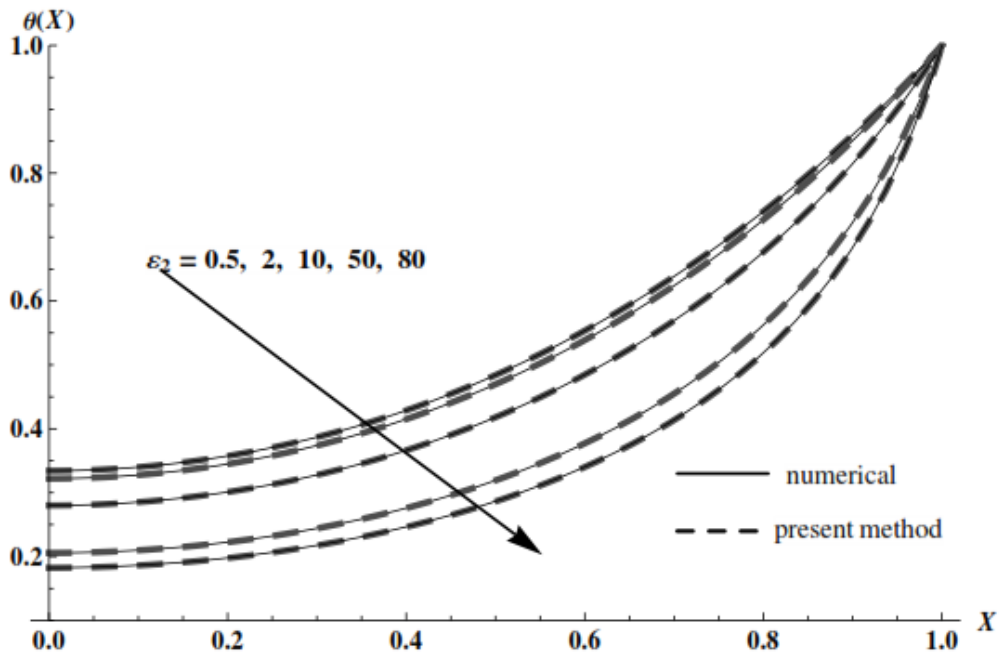


Figure 8 Comparison between the solutions from the used method and numerical solutions for $\theta(X)$ at $N = 2$, $\varepsilon_1 = 0.5$, $M = 15$ and different values of ε_2 .

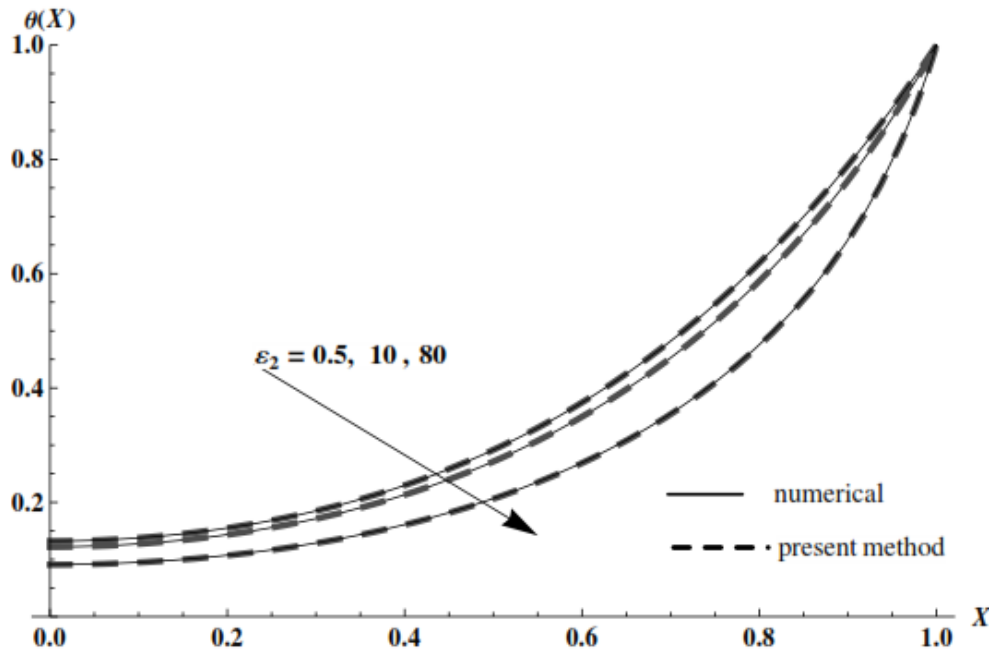


Figure 9 Comparison between the solutions from the used method and numerical solutions for $\theta(X)$ at $N = 3, \epsilon_1 = 0.5, M = 15$ and different values of ϵ_2 .

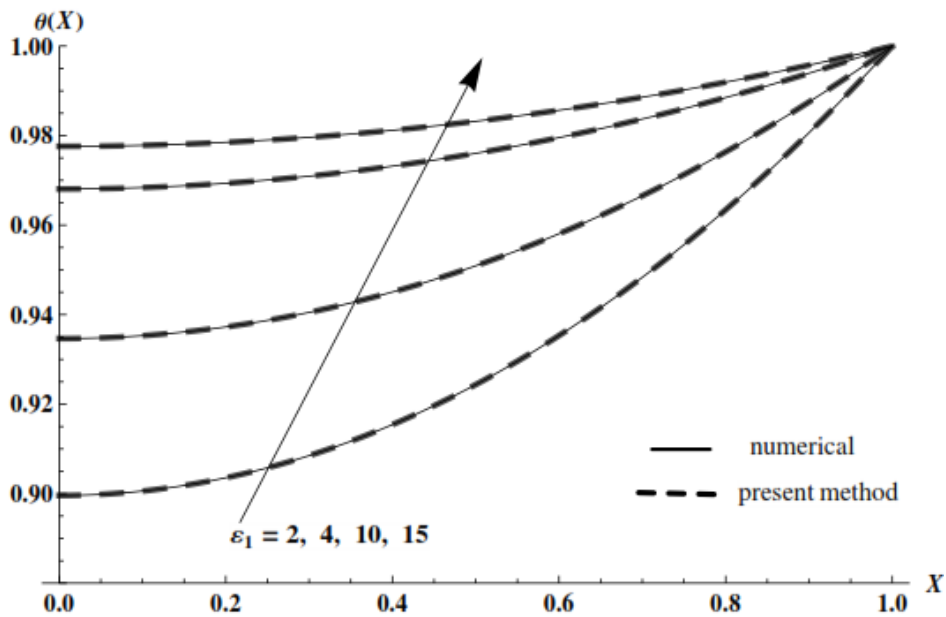


Figure 10 Comparison between the solutions from the used method and numerical solutions for $\theta(X)$ at $N = 0.5, \epsilon_2 = 0.5, M = 15$ and different values of ϵ_1 .

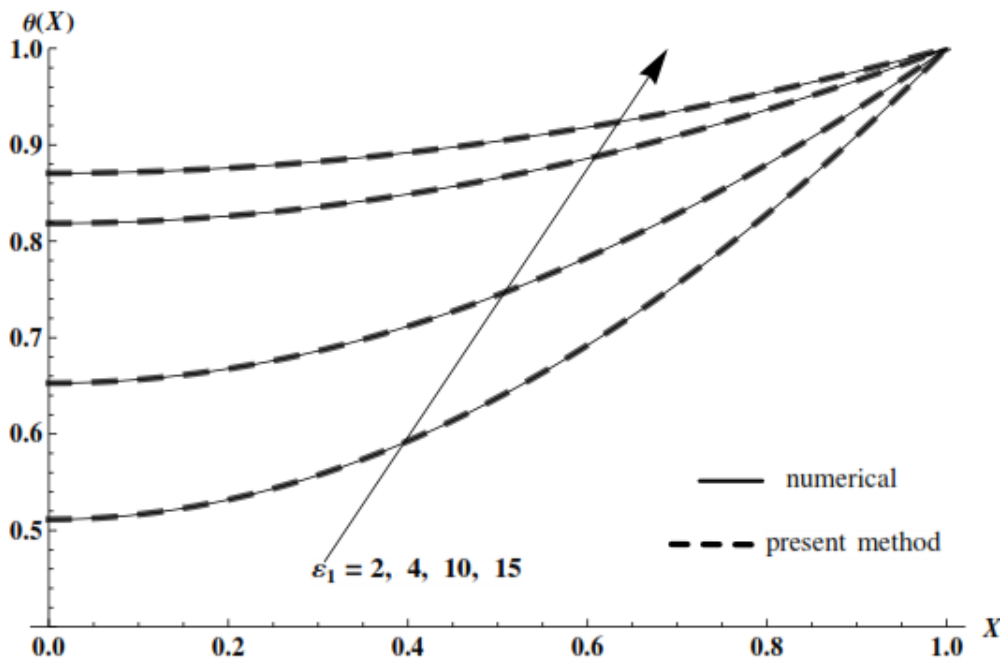


Figure 11 Comparison between the solutions from the used method and numerical solutions for $\theta(X)$ at $N = 2, \varepsilon_2 = 0.5, M = 15$ and different values of ε_1 .

Case (2)

The temperature distribution equation in a thick rectangular fin radiation to free space with the nonlinearity of high order if $\lambda = \gamma = 0, \beta = \varepsilon$ and $u(x) = \theta(x)$ then the problem Eq. (1) becomes;

$$\frac{d^2\theta}{dx^2} - \varepsilon\theta^4 = 0, \theta'(0) = 0, \theta(1) = 1. \tag{45}$$

The approximation solution $\theta(x)$ to Eq. (45) from Eq. (39) becomes;

$$\theta(x) = U_M(x, \hbar, \alpha, \varepsilon) = \sum_{m=0}^M u_m(x, \hbar, \alpha, \varepsilon), \tag{46}$$

From Eq. (40) the relationship between $\alpha = \theta(0)$ and the convergence-control parameter \hbar becomes;

$$\theta(1) \cong U_M(1, \hbar, \alpha, \varepsilon) = 1, \tag{47}$$

The problem Eq. (45) has been successfully solved by the homotopy analysis method (HAM) in [4, 25] for the values of $\varepsilon = 0.7, 1$ and 5 , but in this study, we have successfully solved for large values of ε

and compared the obtained series solution with the exact solution [26]. To find the optimal value of the convergence-control parameter \hbar by minimizing the square residual error Δ_M .

Figures 12 and 13 are $\alpha - \hbar$ curves of Eq. (47) at the orders of approximations $M = 5$ for small values of ε and $M = 15$ for large values of ε , it is easy to discover the valid region of \hbar (R_h) that corresponds to the line segment nearly parallel to the horizontal axis (constant α value) but not get the optimal value from the $\alpha - \hbar$ figures, the value of \hbar can be found by solving Eq. (47) and Eq.(28), the summary of the optimal values of \hbar for different value of ε in **Tables 7 - 8** and are compared with the value of $\theta(0) = \alpha$ from the exact solution [28], from these tables, it is observed that the square residual error, $\Delta_M \cong 0$. **Figure 14** shows the comparison of between the used method and exact solutions for the value of $\theta(0) = \alpha$ at different values of ε . This indicates the high accuracy of the used method.

Table 7 Comparison between exact solutions and used method solutions for value of $\theta(0)$ at $M = 5$ for different values of ε .

$M = 5, K = 100$				
ε	Exact $\theta(0)$ [28]	$\alpha = \theta(0)$	\hbar	Δ_M (26)
0.7	0.8186424	0.8186411	-1.1545	2.398×10^{-10}
1	0.7791451	0.7791403	-1.1980	4.183×10^{-9}
2	0.69431	0.69427	-1.3059	6.861×10^{-7}
5	0.57559	0.57532	-1.4824	0.0002689

Table 8 Comparison between exact solutions and used method solutions for value of $\theta(0)$ at $M = 15$ for different values of ε .

$M = 15, K = 100$				
ε	Exact $\theta(0)$ [26]	$\alpha = \theta(0)$	\hbar	Δ_M (26)
10	0.48838571	0.488385702	-1.4719	1.4983×10^{-10}
20	0.4079422	0.4079419	-1.6059	2.292×10^{-7}
40	0.336474	0.336471	-1.7471	0.000099574138
60	0.299197	0.299186	-1.8299	0.00208519
80	0.274788	0.274768	-1.8873	0.01466
100	0.2570	0.2569	-1.9303	0.059545

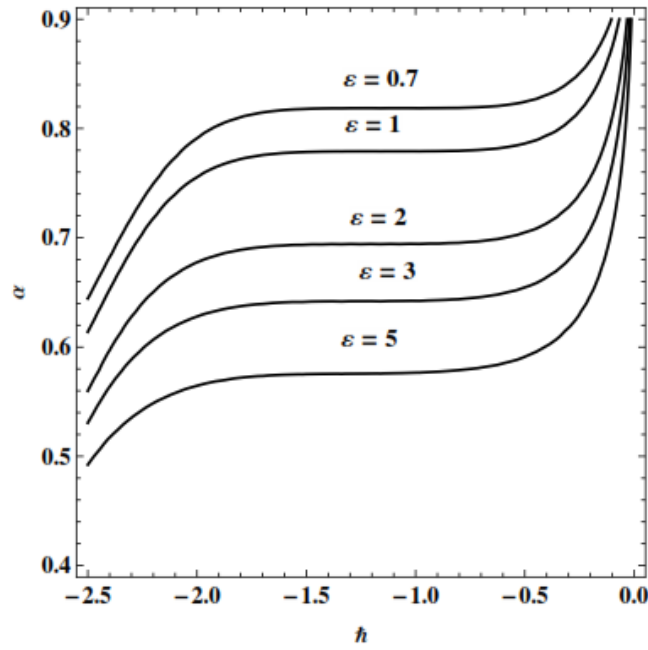


Figure 12 $\alpha - \hbar$ curves of Eq. (47) for different values of ε at $M = 5$.

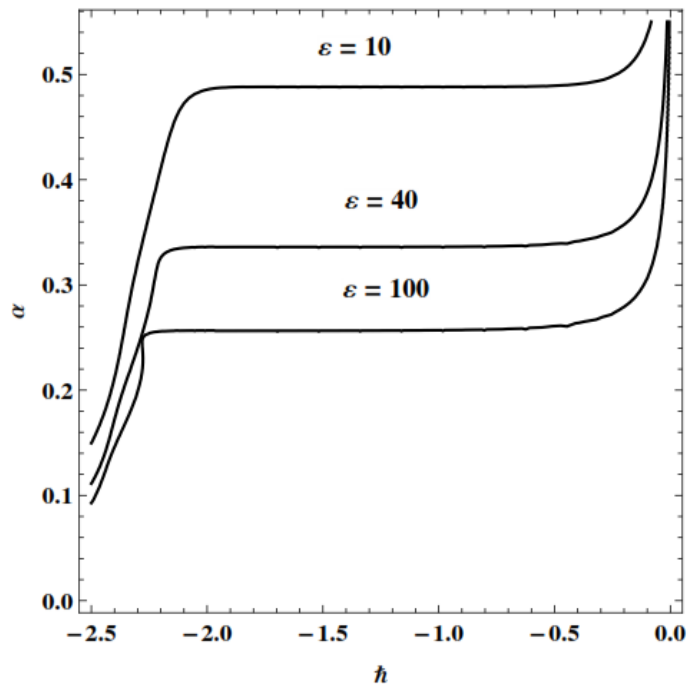


Figure 13 $\alpha - \hbar$ curves of Eq. (47) for different values of ε at $M = 15$.

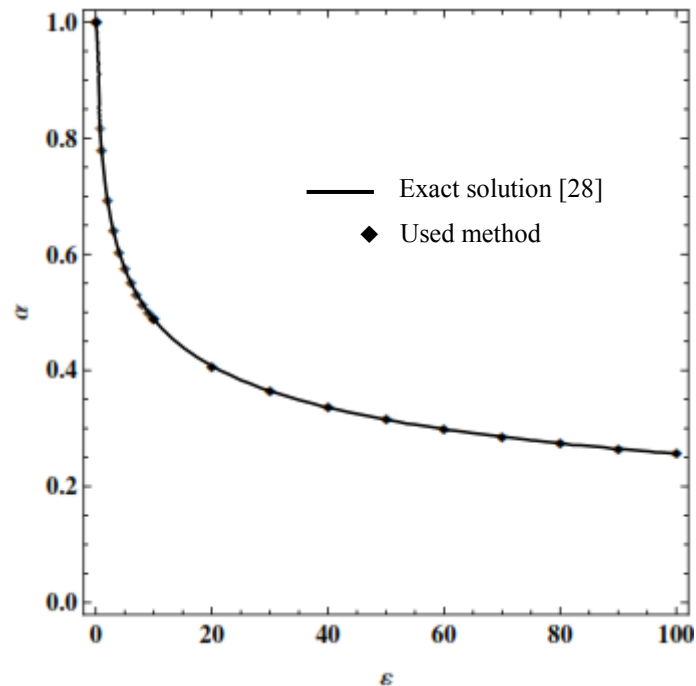


Figure 14 Comparison between the used method and exact solutions for the value of $\theta(0) = \alpha$ at different values of ϵ .

Conclusions

The used method (OHAM) has been successfully solved practical nonlinear two point boundary value problems with strong nonlinear terms and large values of parameters. The figures and tables clearly show the high accuracy of the used method to solve heat transfer problems at different values of important parameters. In addition, the fin efficiency is also accurately evaluated. The optimal value of the convergence controller parameter h can be obtained successfully using the used approach which give the fastest convergence series.

References

- [1] DD Ganji, M Rahimi, M Rahgoshay and M Jafari. Analytical and numerical investigation of fin efficiency and temperature distribution of conductive, convective, and radiative straight fins. *Heat Tran. Asian Res.* 2011; **40**, 233-45.
- [2] DD Ganji and A Rajabi. Assessment of homotopy-perturbation and perturbation methods in heat radiation equations. *Int. Comm. Heat Mass Tran.* 2006; **33**, 391-400.
- [3] DD Ganji. The application of He's homotopy perturbation method to nonlinear equations arising in heat transfer. *Phys. Lett. A* 2006; **355**, 337-41.
- [4] S Abbasbandy. The application of homotopy analysis method to nonlinear equations arising in heat transfer. *Phys. Lett. A* 2006; **360**, 109-13.
- [5] C Arslanturk. A decomposition method for fin efficiency of convective straight fins with temperature-dependent thermal conductivity. *Int. Comm. Heat Mass Tran.* 2005; **32**, 831-41.
- [6] CH Chiu and CK Chen. A decomposition method for solving the convective longitudinal fins with variable thermal conductivity. *Int. J. Heat Mass Tran.* 2002; **45**, 2067-75.

- [7] SB Coskun and MT Atay. Fin efficiency analysis of convective straight fins with temperature dependent thermal conductivity using variational iteration method. *Appl. Therm. Eng.* 2008; **28**; 2345-52.
- [8] SJ Liao. 1992, The Proposed Homotopy Analysis Technique for the Solution of Nonlinear Problems, Ph. D. Thesis. Shanghai Jiao Tong University, China.
- [9] SJ Liao. *Beyond Perturbation: An Introduction to Homotopy Analysis Method*. Boca Raton, Chapman Hall, CRC Press, 2003, p. 22-60.
- [10] SJ Liao. Notes on the homotopy analysis method: Some definitions and theorems. *Comm. Nonlinear Sci. Numer. Simulat.* 2009; **14**, 983-97.
- [11] HN Hassan and MA El-Tawil. A new technique for using homotopy analysis method for second order nonlinear differential equations. *Appl. Math. Comput.* 2012; **219**, 708-28.
- [12] HN Hassan and MA El-Tawil. An efficient analytic approach for solving two-point nonlinear boundary value problems by homotopy analysis method. *Math. Meth. Appl. Sci.* 2011; **34**, 977-89.
- [13] RAV Gorder. Gaussian waves in the Fitzhugh-Nagumo equation demonstrate one role of the auxiliary function $H(x, t)$ in the homotopy analysis method. *Comm. Nonlinear Sci. Numer. Simulat.* 2012; **17**, 1233-40.
- [14] J Biazar and B Ghanbari. HAM solution of some initial value problems arising in heat radiation equations. *J. King Saud Univ. Sci.* 2012; **24**, 161-5.
- [15] B Raftari and K Vajravelu. Homotopy analysis method for MHD viscoelastic fluid flow and heat transfer in a channel with a stretching wall. *Comm. Nonlinear Sci. Numer. Simulat.* 2012; **17**, 4149-62.
- [16] HN Hassan and MM Rashidi. Analytical solution for three-dimensional steady flow of condensation film on inclined rotating disk by optimal homotopy analysis method. *Walailak J. Sci. & Tech.* 2013; **10**, 479-98.
- [17] S Abbasbandy and A Shirzadi. A new application of the homotopy analysis method: Solving the Sturm-Liouville problems. *Comm. Nonlinear Sci. Numer. Simulat.* 2011; **16**, 112-26.
- [18] W Yongyan and KF Cheung. Homotopy solution for nonlinear differential equations in wave propagation problems. *Wave Motion* 2009; **46**, 1-14.
- [19] M Inc. On exact solution of Laplace equation with Dirichlet and Neumann boundary conditions by the homotopy analysis method. *Phys. Lett. A* 2007; **365**, 412-5.
- [20] Z Wang, L Zou and H Zhang. Applying homotopy analysis method for solving differential-difference equation. *Phys. Lett. A* 2007; **369**, 77-84.
- [21] H Jafari and S Seifi. Solving a system of nonlinear fractional partial differential equations using homotopy analysis method. *Comm. Nonlinear Sci. Numer. Simulat.* 2009; **14**, 1962-9.
- [22] SJ Liao. An optimal homotopy-analysis approach for strongly nonlinear differential equations. *Comm. Nonlinear Sci. Numer. Simulat.* 2010; **15**, 2003-16.
- [23] DD Ganji, M Rahgoshay, M Rahimi and M Jafari. Numerical investigation of fin efficiency and temperature distribution of conductive, convective, and radiative straight fins. *Int. J. Res. Rev. Appl. Sci.* 2010; **4**, 9-16.
- [24] M Sajiad and T Hayat. Comparison of HAM and HPM solutions in heat radiation equations. *Int. Comm. Heat Mass Tran.* 2009; **36**, 59-62.
- [25] MSH Chowdhury, I Hashim and O Abdulaziz. Comparison of homotopy analysis method and homotopy-perturbation method for purely nonlinear fin-type problems. *Comm. Nonlinear Sci. Numer. Simulat.* 2009; **14**, 371-8.
- [26] S Abbasbandy and E Shivanian. Exact analytical solution of a nonlinear equation arising in heat transfer. *Phys. Lett. A* 2010; **374**, 567-74.